

N 70 20423

NASA CR100943

# THEORETICAL CHEMISTRY INSTITUTE THE UNIVERSITY OF WISCONSIN

Dissociation Energy and Long-Range Potential of Diatomic Molecules  
from Vibrational Spacings of Higher Levels

by

Robert J. LeRoy and Richard B. Bernstein

WIS-TGI-362

13 November 1969

CASE FILE  
COPY  
MADISON, WISCONSIN

Dissociation Energy and Long-Range Potential of Diatomic Molecules  
from Vibrational Spacings of Higher Levels\*

by

Robert J. LeRoy and Richard B. Bernstein

Theoretical Chemistry Institute and Chemistry Department  
University of Wisconsin, Madison, Wisconsin 53706

ABSTRACT

An expression is derived which relates the distribution of vibrational levels near the dissociation limit  $D$  of a given diatomic species to the nature of the long-range interatomic potential in the region where the latter may be approximated by  $D - C_n/R^n$ . Fitting experimental energies directly to this relationship yields values of  $D$ ,  $n$ , and  $C_n$ . This procedure requires a knowledge of the relative energies and relative vibrational numbering for at least four rotationless levels lying near the dissociation limit; however, it requires no information on the rotational constants, or on the number and energies of the deeply bound levels.  $D$  can be evaluated with a much smaller uncertainty than heretofore obtainable from Birge-Sponer extrapolations. The formula predicts the energies of all vibrational levels lying above the highest one measured, with uncertainties no larger than that of the binding energy of the highest level. The validity of the method is tested with model potentials and its usefulness is demonstrated by application to the precise data of Douglas, Møller, and Stoicheff for the  $B^3\Pi_{Ou}^+$  state of  $Cl_2$ .

-----  
\* Work supported by National Science Foundation Grant GP-7409 and National Aeronautics and Space Administration Grant NGL 50-002-001. R. J. L. acknowledges with thanks the award of a National Research Council of Canada Postgraduate Scholarship.

## I. Introduction

For more than four decades the Birge-Sponer<sup>1</sup> extrapolation procedure has been employed, with only minor modifications,<sup>2,3</sup> for the determination of values for dissociation limits of diatomic molecules from experimental vibrational spacings  $\Delta G_{v+1/2}$ .<sup>4</sup> One of the great virtues of this method is its simplicity, as exemplified by the exact linear relationship between  $\Delta G_{v+1/2}$  and  $v$  for a Morse potential. In this case,  $\Delta G(v)$ <sup>5</sup> extrapolates to zero at  $v_D = (\frac{\omega_e}{2\omega_e x_e} - \frac{1}{2})$ , where  $v_D$  is the non-integer "effective" vibrational index of the dissociation limit.<sup>4</sup> For more realistic potentials it is well known that the Birge-Sponer (B-S) plot shows positive curvature in the region just prior to dissociation, due to the dominating influence of the long-range "tail" of the interatomic potential.<sup>2-4,6</sup> Graphical extrapolation to the dissociation limit is therefore less reliable, and uncertainties greater than  $\pm 10 \text{ cm}^{-1}$  are common in values so obtained for the dissociation limit  $D$ .

The WKB-based method to be described takes advantage of the dominating influence of the long-range portion of the potential on the uppermost vibrational levels. It requires only the energies and relative vibrational numbering of four or more rotationless levels lying close to the dissociation limit  $D$  (ie., less than ca. 10% of the well depth below  $D$ ). These are fitted to an analytical approximation formula, yielding "best" estimates of  $D$  and of the long-range interatomic potential. Although a proper RKR analysis yields a much more accurate estimate of the potential,<sup>7</sup> it is much more restrictive than the present method since it requires as additional information the absolute vibrational numbering, and the energies and  $B_v$  constants of all levels below the one whose turning points are being calculated. Furthermore,

the RKR approach provides no estimate of  $D$  or of the energies or even of the total number of vibrational levels above the highest one observed, and offers no direct means of extrapolating beyond the observed levels.

## II. Method

### A. Derivation and Special Cases

The starting point of the present treatment is the first-order WKB quantum condition for the eigenvalues of a potential  $V(R)$

$$v + \frac{1}{2} = \frac{\sqrt{2\mu}}{\pi\hbar} \int_{R_1(v)}^{R_2(v)} [E(v) - V(R)]^{\frac{1}{2}} dR \quad (1)$$

where  $E(v)$  is the energy of level  $v$ , and  $R_1(v)$  and  $R_2(v)$  are its classical turning points:  $E(v) = V(R_1(v)) = V(R_2(v))$ . Although the allowed eigenvalues correspond to integer  $v$ , it is convenient to treat  $v$  as a continuous variable.

Differentiation of Eq. (1) with respect to  $E(v)$  yields

$$\frac{dv}{dE(v)} = \frac{1}{\pi\hbar} \sqrt{\frac{\mu}{2}} \int_{R_1(v)}^{R_2(v)} [E(v) - V(R)]^{-\frac{1}{2}} dR \quad (2)$$

since the derivatives of the integral limits are zero. Consideration of the nature of the integrand in Eq. (2) suggests that the integral will be very nearly unchanged if the exact  $V(R)$  is replaced by an approximate function which is accurate near the outer turning point  $R_2(v)$ . This is illustrated in Fig. 1 for the case of a model potential, chosen to be of the Lennard-Jones(12,6) form.<sup>8</sup> Using the asymptotic approximation for  $V(R)$  :

$$V(R) = D - C_n/R^n \quad (3a)$$

where  $D$  is the dissociation limit of the potential,  $C_n$  is given by

$$E(v) = D - C_n/[R_2(v)]^n \quad (3b)$$

Changing the variable of integration to  $y \equiv R_2(v)/R$ , Eq. (2) becomes

$$\frac{dv}{dE(v)} = \frac{1}{\pi n} \sqrt{\frac{\mu}{2}} \frac{C_n^{1/n}}{[D-E(v)]^{1/2+1/n}} \int_1^{R_2/R_1} y^{-2} (y^n-1)^{-1/2} dy$$

In the limit  $R_1(v) \rightarrow 0$  (i.e.,  $R_2(v)/R_1(v) \rightarrow \infty$ ) this integral is well known.<sup>3</sup> This yields an approximate analytical expression for  $\frac{dE(v)}{dv}$  near the dissociation limit:

$$\frac{dE(v)}{dv} = \frac{1}{\pi} \sqrt{\frac{2\pi}{\mu}} \frac{\Gamma(1+1/n)}{\Gamma(1/2+1/n)} \frac{n}{C_n^{1/n}} [D-E(v)]^{\frac{n+2}{2n}} = K_n [D-E(v)]^{\frac{n+2}{2n}} \quad (4)$$

where  $K_n$  is an obvious collection of constants and  $\Gamma(x)$  is the gamma function.<sup>10</sup> Note that  $\frac{dE(v)}{dv}$  is closely related to the conventional Birge-Sponer ordinate;<sup>5</sup> c.g.s. units are implied throughout.

Eq. (4) shows that for the uppermost vibrational levels of a given diatomic species, the spacings depend only upon the long range potential parameters  $D$ ,  $n$  and  $C_n$ . Thus, for electronic states with the same long range potential, B-S plots for levels near  $D$  will be precisely superimposable upon shifting of their abscissa ( $v$ ) scales. This result is discussed further in Appendix A.

For sets of vibrational levels which can be described by Eq. (4), the curvature of the B-S plot must be positive, since<sup>5</sup>

$$\begin{aligned} \frac{d^3 E(v)}{dv^3} &= \frac{n+2}{n^2} K_n^3 [D - E(v)]^{3/n - 1/2} \\ &= \frac{d^2 \Delta G(v)}{dv^2} \approx \frac{1}{2} \frac{d^2 (\Delta G_{v-1/2} + \Delta G_{v+1/2})}{dv^2} \end{aligned} \quad (5)$$

For  $n = 6$  this curvature is a constant; for  $n > 6$  it increases with increasing  $v$ , becoming infinite at the dissociation limit; for  $n < 6$  it decreases to zero at  $D$ . Positive curvature of a B-S plot for a set of experimental vibrational energies is therefore a necessary (though not sufficient) condition for the applicability of the present method.

In practical applications it is most convenient to employ the integrated form of Eq. (4),<sup>11</sup> which for  $n \neq 2$  is

$$D - E(v) = \left[ K_n \left( \frac{n-2}{2n} \right) (v_D - v) \right]^{\frac{2n}{n-2}} \quad (6)$$

where, in general,  $v_D$  is an integration constant.<sup>12,13</sup> For  $n > 2$ ,  $v_D$  takes on physical significance as the effective (non-integer) vibrational index at the dissociation limit, provided that the potential is well approximated by Eq. (3) from the highest observed levels up to  $D$ . In this case, truncation of  $v_D$  to an integer yields the vibrational index of the uppermost rotationless level, say  $N_D$ . It is interesting to note that the "natural" dependent and independent variables in Eq. (6) are respectively the binding energy  $D - E(v)$ , and the vibrational "index" counted down from  $D$  (for  $n > 2$ ). Applications of the present method are based upon the

fitting of experimental energies  $E(v)$  to Eq. (6) to yield values of the four quantities  $D$ ,  $n$ ,  $C_n$  and  $v_D$ . This is discussed further in Sec. IIC and III.

While the potentials considered above ( $n > 2$ ) are of most practical interest, results for  $n < 2$  will be noted. Here the integration constant  $v_D$  must be smaller than any of the  $v$  values of the levels being fitted (and may even be negative), since  $K_n$  is positive and  $(n-2)$  is negative (see Eq. (6)). For  $n = 1$ , Eq. (6) becomes

$$D - E(v) = \frac{\mu}{2\hbar^2} \frac{C_1^2}{(v-v_D)^2}$$

which is the exact quantum result if one sets  $v_D = -1$ .<sup>14</sup> For  $n = 2$ , integration of Eq. (4) yields

$$D - E(v) = [D - E(0)] \exp \left[ -\pi \hbar v \sqrt{\frac{2}{\mu C_2}} \right] \quad (7)$$

Here the assignment of any given level as  $v = 0$  is arbitrary since the levels cannot be enumerated either down from  $D$  or up from a lowest level.<sup>15</sup> Eq. (7) is identical to the exact quantal result<sup>14</sup> except that it omits the (usually small) effect on the apparent  $C_2$  constant of the Langer correction<sup>16</sup> to the WKB integral, Eq. (1).

The present approach can also be applied to potentials whose long-range tails are not of the inverse power form. For example, consider any potential with an attractive exponential tail,<sup>17</sup> such that at large  $R$ :  $V(R) = D - Ae^{-\beta R}$ . Applying the same approximations (replacing the full potential in Eq. (2) by its tail, and letting  $R_1 \rightarrow 0$ ), an expression analogous to Eq. (4) is obtained:

$$\frac{dE(v)}{dv} = \sqrt{\frac{2}{\mu}} \hbar \beta \left[ D - E(v) \right]^{\frac{1}{2}} \left[ 1 - \frac{2}{\pi} \sin^{-1} \sqrt{\frac{D-E(v)}{A}} \right] \quad (8)$$

As with Eq. (4), in this case the vibrational spacings near  $D$  depend only on the potential parameters (here  $D$ ,  $\beta$ , and  $A$ ) and to a first approximation (ignoring the arcsin term) they are independent of  $A$ . Integration of this expression yields

$$\sqrt{\frac{D-E(v)}{A}} \left[ 1 - \frac{2}{\pi} \sin^{-1} \sqrt{\frac{D-E(v)}{A}} \right] + \frac{2}{\pi} \left[ 1 - \sqrt{1 - \frac{D-E(v)}{A}} \right] = \frac{\hbar \beta}{\sqrt{2\mu A}} (v_D - v)$$

where the integration constant  $v_D$  has the same physical significance as in the inverse power ( $n > 2$ ) case. Upon expanding the left hand side as a power series in  $\sqrt{\frac{D-E(v)}{A}}$ , reversion of the series yields

$$D-E(v) = \frac{\hbar^2 \beta^2}{2\mu} (v_D - v)^2 \left[ 1 + (v_D - v) Y + \frac{5}{4} (v_D - v)^2 Y^2 + \cdots \right] \quad (9)$$

where

$$Y = \sqrt{\frac{2}{\mu A}} \frac{\hbar \beta}{\pi} \quad (10)$$

As with the inverse power potential, the B-S plot will show positive curvature; however here the curvature is quite small and to first order (setting  $Y=0$ ) it is zero.<sup>18</sup>

This result (Eq. (9)) for potentials with an exponential tail is particularly useful since it allows a test of the approximations underlying the present treatment. One may compare Eq. (9) with the exact quantum results for one realistic model potential with an exponential tail,

the Morse potential:<sup>19</sup>  $V_M(R) = D_e \left[ 1 - e^{-\beta(R-R_e)} \right]^2$ , whose eigenvalues are given by<sup>4,14</sup>

$$D-E(v) = \frac{\hbar^2 \beta^2}{2\mu} (v_D - v)^2 = \omega_e x_e (v_D - v)^2 \quad (11)$$

where  $v_D$  is, as before, the effective vibrational index at  $D$ . Clearly, in the limit  $Y \rightarrow 0$ , the distribution of vibrational levels predicted by Eq. (11) agrees with that of Eq. (9). This is true despite the change in  $v_D$ , which merely amounts to a change in vibrational numbering and a small shift in the eigenvalues (arising from the small change in  $v_D - N_D$ ); in effect this change in  $v_D$  merely shifts the abscissa scale in the B-S plot. The influence of the short-range portion of the Morse potential is thus merely to remove the small "correction" terms in  $(v_D - v)Y$  from Eq. (9), yielding Eq. (11). The value of  $Y$  depends on both  $\beta$  and the coefficient of the long range (attractive) exponential term in  $V_M(R)$ ,  $2D_e e^{\beta R}$ ; substituting this for  $A$  in Eq. (10) and using known relations among the Morse parameters<sup>4</sup> one identifies

$$Y = \frac{\sqrt{8}}{\pi} \frac{\omega_e x_e}{\omega_e} e^{-\frac{1}{2}\beta R_e} \quad (12)$$

which shows that for typical diatomics  $Y \ll 1$ .

### B. Significance of Parameters and Sources of Error

Perturbation theory suggests<sup>20</sup> that near the dissociation limit the internuclear interaction may be expressed as a sum of inverse (integer) power terms in  $R$ :

$$V(R) = D - \sum_m C_m / R^m \quad (13)$$

Over any small interval, Eq. (3) is a close approximation to Eq. (13), if one considers  $n$  to be an "effective" or "local" power which corresponds to a weighted average of the different  $m$  values:<sup>21</sup>

$$n = \frac{\sum_m (m+1) C_m / R_2(v)^{m+1}}{\sum_m C_m / R_2(v)^{m+1}} - 1 \quad (14)$$

In the limit  $v \rightarrow v_D$ , as  $R_2(v)$  reaches the asymptotic region, the effective non-integer power  $n \rightarrow \tilde{n}$ , the (integer) smallest power contribution to Eq. (13). As long as the potential for the state in question is well behaved,<sup>22</sup> fits of Eq. (6) to different subsets of a given energy spectrum should all yield essentially the same value of  $D$ , though the "local" values of  $n$ ,  $C_n$  and  $v_D$  differ slightly.

At somewhat shorter separations, exponential-type exchange forces replace the inverse-power terms in dominating the interaction;<sup>20</sup> thus, the B-S plot becomes increasingly linear for the deeper levels.<sup>18</sup> However, the approximations of the present treatment are worse for these more deeply bound levels, so only the region dominated by the long-range inverse-power terms (positive curvature of the B-S plot) should be treated by the present method.

There are two main sources of error inherent in the approximations represented by Eq. (3). First and most obvious is the neglect of the singularity at  $R_1(v)$  in the exact integrand of Eq. (2) (see Fig. 1). This omission tends to make the estimate of the integral used to obtain Eq. (4) somewhat small, and since the relative magnitude of this error

decreases for the higher levels, the effect will be to yield values of both  $n$  and  $C_n$  which are somewhat too large.

The second source of error arises from the fact that a realistic long-range interatomic potential is a sum of attractive inverse-power terms (see Eq. (13)) in contrast to the single attractive term in the model L.J.(12,6) potential. This means that whatever the effective inverse-power precisely at a given  $R_2(v)$  (from Eq. (14)), terms with higher powers contribute relatively more to the potential for  $R < R_2(v)$ , so that the exact integrand of Eq. (2) is smaller than that for the single  $C_n/R^n$  function which best fits the potential at  $R_2(v)$ . This error has the opposite effect of the first, tending to produce values of  $n$  and  $C_n$  which are slightly too small. The former error is most serious for the deeper levels, while the latter dominates the situation as  $n$  (see Eq. (14)) approaches its asymptotic value  $\tilde{n}$ .<sup>23</sup>

A third potential source of error arises from use of the first-order WKB approximation (given by Eq. (1)), compounded by the omission of the Langer correction.<sup>16</sup> However the effect of this approximation is expected to be negligible.<sup>24</sup>

Values of  $D$ ,  $n$  and  $C_n$  obtained on fitting any given set of vibrational energies to Eq. (6) yield a "local" estimate of the potential in the form of Eq. (3). Because of the errors described above, this estimate of the potential will be somewhat too deep when using data for the deeper levels, and slightly too shallow when considering only the highest levels. This is illustrated by the examples considered in Sec. III.

Next in importance to  $D$  are the power  $\tilde{n}$  and coefficient  $C_{\tilde{n}}$  of the longest range (lowest power) term in the expansion for the potential

(see Eq. (13)). The errors in  $n$  (see above) which induce slight errors in  $D$ , may also weaken the accuracy of  $\tilde{n}$ . However, for many electronic states  $\tilde{n}$  is known from theoretical considerations;<sup>25</sup> the only question is whether the levels being fitted lie close enough to the dissociation limit  $D$  to be governed mainly by the asymptotic  $R^{-\tilde{n}}$  term of the potential. If this is so, it is desirable to constrain  $n$  to be equal to  $\tilde{n}$  and employ a three parameter fit to Eq. (6) (or if  $\tilde{n} = 2$ , a two parameter fit to Eq. (7)). This should yield improved accuracy in  $D$  and provide significant values of the theoretically interesting  $C_{\tilde{n}}$  and  $v_D$ .

### C. Implementation

In this section, a procedure is described for the practical application of the present method to experimental data in a manner intended to yield the best possible estimates of the parameters  $D$ ,  $n$ ,  $C_n$  and (for  $n \neq 2$ )  $v_D$ . The general case of  $n \neq 2$  will be considered first, followed by a brief discussion of the situation for  $n = 2$ .

A least-squares fit of experimental energies directly to Eq. (6) is the most general way of obtaining the best values of the four quantities;<sup>26</sup> However, since this expression is non-linear in the parameters, the general regression problem may have no unique solution since the sum of squares may show local minima which do not correspond to the best parameter values. This problem can be avoided if the initial trial parameter values required by non-linear regression procedures are sufficiently accurate. The necessary trial values for  $n$  and  $v_D$  may be obtained from a fit to a linear expression obtained on combining

derivatives from Eq. (6):<sup>27</sup>

$$E'(v)/E''(v) = - \left( \frac{n-2}{n+2} \right) (v_D - v) \quad (15)$$

Holding fixed the  $n$  and  $v_D$  values thus obtained, Eq. (6) becomes linear in a new independent variable,  $w \equiv \left[ \left( \frac{n-2}{2n} \right) (v_D - v) \right]^{\left( \frac{2n}{n-2} \right)}$ :

$$E(v) = D - w K_n^{\left( \frac{2n}{n-2} \right)} \quad (16)$$

This yields trial values of  $D$  and  $K_n$  (which gives  $C_n$  via Eq. (4)), The four parameter values thus obtained are good starting approximations for the direct non-linear fit of the experimental energies to Eq. (6);<sup>28</sup> the linearity of Eq. (15) and (16) makes this approach particularly straightforward.<sup>29,30</sup>

While Eq. (16) may be used only for  $n \neq 2$ , Eq. (15) is also valid for  $n = 2$ , since combining the derivatives of Eq. (7) shows that

$$\frac{E'(v)}{E''(v)} = \frac{-1}{\pi\hbar} \sqrt{\frac{\mu C_2}{2}}$$

Thus, even though  $v_D(n=2) = \infty$ ,  $\lim_{n \rightarrow 2} \left( \frac{n-2}{n+2} \right) v_D(n) = \frac{1}{\pi\hbar} \sqrt{\frac{\mu C_2}{2}}$ . Manipulating Eq. (4) and its derivatives, one obtains simple expressions yielding trial values of  $D$  and  $C_n$ :

$$D = E(v) - \left( \frac{n+2}{2n} \right) \frac{[E'(v)]^2}{E''(v)} \quad (17a)$$

and

$$K_n = E'(v) / [D - E(v)]^{\left( \frac{n+2}{2n} \right)} \quad (17b)$$

where, as before,  $C_n$  is obtained from  $K_n$ . While Eqs. (17) are valid for all  $n$ , in practice they are somewhat less accurate and more difficult to use than is Eq. (16).<sup>31</sup>

### III. Applications

#### A. Dissociation Limit and Potential Tail from Eigenvalues of a Model Potential

The method is first applied to the exact eigenvalues of the previously mentioned (Sec. IIA) 24-level L.J.(12,6) potential:<sup>8</sup>

$$V(R) = 1 + 1/R^{12} - 2/R^6 \quad (\text{here } D = 1, \tilde{n} = 6, C_6 = 2).$$

A B-S plot of the eigenvalues of any L.J.(12,6) potential has positive curvature everywhere.<sup>6</sup> However, as discussed in Sec. II, consideration of the deeper levels by the present method is inappropriate, so the following analysis deals only with the eleven levels lying less than 10% of the well depth below the dissociation limit (i.e.,  $D - E(v) \leq 0.1 D_e$ ).<sup>19</sup> Throughout this section, energies are expressed in units of the well depth (i.e., set  $D_e = 1$ ), length in units of the equilibrium distance (i.e., set  $R_e = 1$ ), and the zero of energy is set at the potential minimum.

The calculated eigenvalues<sup>8</sup> for the eleven highest levels were smoothed by fitting them to a 5<sup>th</sup> order polynomial in  $v$ , in order to obtain the derivatives on the left hand side of Eq. (15). Fig. 2 shows a plot of this derivative ratio vs.  $v$ , compared with lines whose slopes correspond (via Eq. (15)) to integer  $n = 5, 6$ , and  $7$ .<sup>32</sup> A least squares fit of these derivative ratios to Eq. (15) yielded  $n = 6.29$  and  $v_D = 23.27$ ;<sup>32</sup> fixing  $n$  and  $v_D$  at these values, a subsequent fit of the

eigenvalues to Eq. (16) yielded  $D = 1.0 - 1.31 \times 10^{-5}$  (the correct value is exactly 1.0) and  $C_n = 3.43$ . These estimates of the parameters were then used as the initial trial values for a non-linear fitting of the eleven energies to Eq. (6).<sup>26,29</sup> The parameters thus obtained were  $D = 1.0 - 1.29 \times 10^{-5}$ ,  $n = 6.30$ ,  $C_n = 3.46$  and  $v_D = 23.25$ .

The above fitting procedure was then repeated several times while the deeper levels were successively omitted. Levels in the interval  $v_L \leq v \leq v_H$  were included in a given fit;  $v_H$  was fixed at 23 (the highest level) while  $v_L$  was successively increased from 13 to 19.<sup>33</sup> In Fig. 3 the resulting parameter values (solid curves) are plotted against the energy of the lowest level included in a given fit,  $E(v_L)$ .

For a L.J.(12,6) potential  $\tilde{n} = 6$  and the effective  $n$  at the outer turning point (from Eq. (14)) is always less than six ; thus the fact that four-parameter fits to Eq. (6)<sup>29</sup> always yield  $n > 6$  must be due to the first source of error discussed in Sec. IIB.

To obtain more accurate estimates of  $D$ ,  $C_n$  and  $v_D$ , the above fitting procedure was repeated with  $n$  fixed at  $\tilde{n} = 6$ . Levels  $v_L$  to  $v_H = 23$  were fitted while  $v_L$  was increased successively from 13 to 20,<sup>29,33</sup> yielding the parameter values joined by the dashed curves in Fig. 3. This procedure was repeated with  $n$  fixed in turn at 5 and 7, yielding the dotted curves in Fig. 3. Consideration of the different curves for  $D$  suggests that their comparative convergence (flattening) is a test of the true value of  $\tilde{n}$ .<sup>34</sup> In general, the three-parameter fits with  $n$  fixed at  $\tilde{n}$  yield meaningful values of  $C_{\tilde{n}}$  and  $v_D$  and give better estimates of  $D$  than do the four-parameter fits. "Best" values of all parameters are obtained from the right hand ends of the dashed curves in

Fig. 3:  $D = 1.0 \pm 0.13 \times 10^{-5}$ ,  $C_6 = 2.01$ , and  $v_D = 23.353$ . This  $v_D$  value agrees well with the first order WKB value of 23.358.<sup>35</sup>

As pointed out above, the dominant error affecting these L.J.(12,6) results arises from the effect of the singularity at  $R_1(v)$ . The values of  $n$  and  $C_n$  obtained from the four-parameter fits (and the  $C_6$  values from the three-parameter fits) are somewhat large; as expected, the error diminishes as the deeper levels are successively dropped.

As discussed in Sec. IIB, the present method yields values of  $D$ ,  $n$  and  $C_n$  which provide "local" estimates of the potential over the range of energies being fitted. Hence the outer tail of the potential may be approximated by the results of a series of piecewise fits. Furthermore, since all of the pieces should correspond to the same value of  $D$ , holding  $D$  fixed at the "best" value obtained above should improve the accuracy of the derived potential, particularly for the deeper segments. To explore this point, levels  $v_L$  to  $v_H$  were fitted to Eq. (6),<sup>29</sup> with  $D$  held fixed at 1.0 and  $v_H - v_L = 4$ , while  $v_H$  was successively decreased from 23 to 17. The resultant "local" curves are shown in Fig. 4 (only the segments corresponding to odd  $v_H$  have been included); the points are the exact turning points, and in this region are indistinguishable from the  $-2/R^6$  asymptotic tail. As expected, the fitted segments are somewhat too deep. However the "nesting" of the successive segments shows the decreasing error in the fitted  $n$  and  $C_n$  as the dissociation limit is approached.<sup>23</sup>

### B. Dissociation Limit and Potential Tail of $\text{Cl}_2(\text{B}^3\Pi_{0u}^+)$

The method is now applied to experimental data for the  $\text{B}^3\Pi_{0u}^+$  state of  $\text{Cl}_2$ . Douglas, Møller and Stoicheff<sup>36</sup> have reported accurate vibrational energies of levels  $v = 6$  to 31 of this state, the highest observed level lying only a few  $\text{cm}^{-1}$  below  $D$ . A B-S plot of their data shows positive curvature above  $v = 11$ , and hence these higher levels may be treated by the present method. In what follows, the zero of energy is conveniently set at the lowest vibrational-rotational level of the ground ( $\text{X}^1\Sigma_g^+$ ) electronic state; results are reported in the conventional spectroscopic energy and length units:  $\text{cm}^{-1}$  and  $\text{\AA}$ .<sup>37</sup>

As in the L.J.(12,6) case, the vibrational energies<sup>36</sup> were repeatedly fitted to Eq. (6) (with four free parameters)<sup>26,29,33</sup> while the deeper levels were successively omitted from consideration, yielding the values of  $n$  shown in Fig. 5. Theory indicates<sup>38</sup> that  $\tilde{n} = 5$  for this state. The fact that the fitted  $n$  falls slightly below 5 (for  $v_L = 26$  and 27) is probably due to the second type of error discussed in Sec. IIB. Over the region where the fitted  $n \lesssim 5$ , the eigenvalue distribution is probably dominated by the  $R^{-5}$  term in the potential. In view of this, the data were refitted to Eq. (6) with  $n$  held fixed at 5,<sup>26,29,33</sup> to yield the estimates of  $D$ ,  $C_n$  and  $v_D$  joined by the dashed lines in Fig. 5. These ( $n=5$ ) values of  $D$  are also compared to those obtained from analogous fits with  $n$  fixed respectively at 4 and 6 (dotted curves). A comparison of the limiting ( $E(v_L) \rightarrow D$ ) behavior of the three  $D$  curves for fixed  $n$  supports the conclusion that the highest five or six levels lie in the asymptotic  $\tilde{n} = 5$  region. Furthermore, comparison of the  $n = 5$  and "n free" curves suggests that

the former gives the more reliable estimate of  $D$ . This determination of  $\tilde{n} = 5$  for this state (in agreement with theory) differs with the conclusion of Byrne, Richards, and Horsley;<sup>39</sup> the source of the error in the earlier work is discussed in Ref. 30.

The present analysis yields  $D=20879.75(\pm 0.10)\text{cm}^{-1}$ ,  $C_5=1.29(\pm 0.03)\times 10^5\text{cm}^{-1}\text{\AA}^5$ , and  $v_D(n=5) = 34.90(\pm 0.03)$ .<sup>40</sup> This value of  $D$  is in agreement with, but is considerably more precise than the experimenters' best estimate<sup>36</sup> of  $D = 20880(\pm 2.0)\text{cm}^{-1}$ . The above  $C_5$  compares well with the theoretical value<sup>41</sup> of  $1.4_4 \times 10^5\text{cm}^{-1}\text{\AA}^5$ . Furthermore, the fitted value of  $v_D$  implies that there exist at least three unobserved bound levels above  $v = 31$ . Table I lists the predicted level energies, obtained by substituting  $n = 5$  and the above values for the other three constants into Eq. (6).

Table I. Calculated energies (in  $\text{cm}^{-1}$ ) for unobserved bound  $\text{Cl}_2(\text{B}^3\Pi_{0u}^+)$  levels.<sup>37</sup>

$v$	32	33	34
$E(v)$	20878.69	20879.49	20879.73

It is interesting to explore the question of the accuracy of the  $D$  value which would have been obtained by the present method if the data for a few of the highest observed levels had not been available. In this case the local potential for the highest remaining levels would not be dominated by the asymptotic  $R^{-\tilde{n}}$  ( $\tilde{n}=5$ ) term, so general four-parameter fits to Eq. (6) are necessary (cf. the three-parameter,  $n$  fixed at  $\tilde{n}$

fits described above). Experimental energies were repeatedly fitted to Eq. (6), eight at a time, as the highest observed levels were successively dropped from consideration.<sup>26,29,33</sup> Fig. 6 shows the values of  $D$  so obtained plotted vs. the energy of the highest level included in a given fit  $E(v_H)$ .<sup>42</sup> It is noted that even if no levels had been observed above  $v = 20$  (which lies ca.  $244 \text{ cm}^{-1}$  below  $D$ ), the present method would have yielded  $D$  within  $5.5 \text{ cm}^{-1}$ ! In contrast, a linear B-S extrapolation from  $v = 20$  yields an error in  $D$  of ca.  $69 \text{ cm}^{-1}$ .

To obtain an estimate of the tail of the  $\text{Cl}_2(\text{B}^3\Pi_{0u}^+)$  potential curve, the data were again fitted to Eq.(6)<sup>29</sup> eight levels at a time, except this time  $D$  was held fixed at the "best" value of  $20879.75 \text{ cm}^{-1}$ .<sup>43</sup> In Fig.7 the segmented potential so obtained is compared to the RKR turning points calculated by Todd, Richards, and Byrne.<sup>44</sup>

#### IV. Concluding Remarks

It has been shown that the distribution of vibrational levels near the dissociation limit of a diatomic molecule is governed mainly by the long-range attractive tail of the internuclear potential.<sup>45</sup> A simple approximate analytic expression has been derived for this distribution, in terms of the dissociation limit  $D$ , the power  $n$  and coefficient  $C_n$  of the effective local inverse-power potential, and an integration constant  $v_D$  (which has physical significance if  $n = \tilde{n}$ ). These quantities may be determined via a least-squares fit of experimental vibrational energies to this equation.<sup>26,29,33</sup>

This approach yields the binding energy of the highest observed level with an error of at most a few percent, which is far superior to the error often resulting from use of the customary B-S extrapolation

procedures.<sup>3</sup> It also leads to a determination of the power  $n$  and coefficient  $C_n$  of the asymptotically dominating lowest power term in the inverse-power expansion for the potential; the results for  $\text{Cl}_2(\text{B}^3\Pi_{0u}^+)$  accord well with theory.<sup>46</sup> In addition, one obtains an estimate of the outer branch of the potential over the range of the highest levels, albeit less accurate than an RKR potential.<sup>7</sup> However the present method is much less restrictive in its data requirements, and hence may be applied in many situations where the RKR approach cannot. Here the only restrictions on the input data are that the levels must lie near the dissociation limit  $D$ , and that their B-S plot show positive curvature.<sup>47</sup>

A useful additional feature of the present method is its ability (when  $n \approx \tilde{n}$ ) to predict the energies of all unobserved levels lying above the highest observed level.

The main alternative methods of obtaining estimates of  $D$  from spectroscopic data are through use of the less accurate B-S extrapolation (referred to earlier) or from the limiting curve of dissociation (LCD).<sup>3,4</sup> In the latter case,  $D$  is deduced by extrapolation to zero  $J$  of plots of the uppermost observed rotational levels vs.  $J(J+1)$ . A large uncertainty in  $D$  is introduced by the problem of determining the breaking-off point  $J_{\text{max}}$  for each  $v$ ; this is particularly important for the vibrational levels predissociating at small  $J$ , closest to the intercept of the LCD at  $D$  (eg., see the case of  $\text{Br}_2(\text{B}^3\Pi_{0u}^+)$  discussed in Ref. 30). It appears that the LCD method is less reliable than the present one.

Alternative spectroscopic approaches to the determination of  $\tilde{n}$  and  $C_n$  are the standard RKR procedure, and the predissociation method of Bernstein.<sup>48</sup> Difficulties in the use of the former are discussed in Ref. 30.

The latter has been found to yield reasonable results for a number of systems;<sup>38,48,49</sup> however it suffers from the above-mentioned problem of determining  $J_{\max}$ . Furthermore, it presupposes an accurate value of  $D$ . In general, therefore,  $\tilde{n}$  and  $C_{\tilde{n}}$  values extracted from predissociation data are expected to be less reliable than those obtainable by the present method.

In addition to spectroscopic methods, atomic beam scattering measurements yield  $\tilde{n}$  and  $C_{\tilde{n}}$  values of roughly the same accuracy as those obtained from the present method.<sup>50</sup> These two techniques are essentially complementary. The present approach is best applied to electronic states of a strongly ("chemically") bound molecule with many vibrational levels, where the profusion of electronic states arising from the interaction of all but closed-shell atoms precludes the use of scattering measurements. On the other hand, the shallow van der Waals potential wells normally encountered with closed-shell atoms, ideal for study by the beam scattering technique, do not support enough bound states to be treated by the present method.

The new approach has been demonstrated by applying it to the exact computed eigenvalues of a model L.J.(12,6) potential, and to the accurate experimental vibrational energies of  $\text{Cl}_2(\text{B}^3\Pi_{0u}^+)$ . In a companion paper, it is applied<sup>30</sup> to the ground  $(\text{X}^1\Sigma_g^+)$  state of  $\text{Cl}_2$  and to the  $\text{B}^3\Pi_{0u}^+$  states of  $\text{Br}_2$  and  $\text{I}_2$ , and appears to be of quite general utility.<sup>51</sup>

## V. Acknowledgment

The authors appreciate some relevant comments on interatomic forces by Professor J. O. Hirschfelder. They also acknowledge some early correspondence between R. B. B. and Dr. C. L. Beckel and discussions with Dr. H. Harrison, which helped pave the way for the present approach.

Appendix A: Birge-Sponer Plots for Different Potentials with  
Identical Long-Range Tails

The basis of the present method is the conclusion (Eq. 4) that near the dissociation limit  $D$ , the density of vibrational levels  $\frac{dv}{dE(v)}$  is determined almost solely by the nature of the outer (attractive) branch of the potential. Thus, B-S plots (scaled, when necessary by  $\sqrt{U}$ ; see Eq. (4)) of the level spacings for different potentials with identical long-range tails (but with arbitrarily different short-range behavior) will be identical near the dissociation limit, provided their abscissa ( $v$ ) scales are shifted appropriately relative to one another. This may be tested either by using exact (quantal) eigenvalues for suitably chosen potentials, or, with little loss in accuracy, by the use of WKB-approximated eigenvalues. The latter procedure has been employed here. Reduced WKB integral tables are available for L.J.(12,6) and  $\exp(\alpha,6)$  ( $\alpha = 12.0, 13.772$  and  $15.0$ ) potentials.<sup>6,52</sup> The L.J.(12,6) potential considered in these comparisons<sup>8</sup> is that utilized in Sec. IIIA; throughout the present Appendix, all energies and lengths are scaled relative to its well depth and equilibrium distance, and the reduced mass  $\mu$  is assumed to be the same.

For an  $\exp(\alpha,6)$  potential with the same long-range  $R^{-6}$  tail as the model L.J.(12,6),<sup>8</sup>

$$C_6 = 2 = \frac{D_e R_e^6}{(1 - 6/\alpha)} \quad (A1)$$

For any choice of  $D_e$ , Eq. (A1) defines the corresponding  $R_e$ ; the appropriate  $B_z$  value<sup>6</sup> is then obtained by multiplying the  $B_z (=10000.)$

for the model L.J.(12,6) potential<sup>8</sup> by  $D_e R_e^{-2}$ . The parameters of the chosen  $\exp(\alpha,6)$  potentials are given in Table A1.

Table A1. Parameters of  $\exp(\alpha,6)$  Potentials Having Same Long-Range Tail as the Model L.J.(12,6).<sup>8</sup>

Case	E	C	B
$\alpha$	12.0	13.772	15.0
$D_e$	1.0	1.5	2.0
$R_e$	1.0	0.953701	0.918386
$B_z$	10000.0	13643.20	16868.65

For L.J.(12,6) and  $\exp(\alpha,6)$  potentials with  $\alpha = 12.0, 13.772$ , and 15.0, the WKB integral tables<sup>6,52</sup> (based on a reduced form of Eq. (1)) are presented as values of  $\phi = (v+1/2)/\sqrt{B_z}$  vs.  $K \equiv -(D-E(v))/D_e$  and  $\theta \equiv (j+1/2)^2/B_z$ . Thus<sup>5</sup>

$$\Delta G(v) = \frac{D_e}{\sqrt{B_z}} \frac{dK}{d\phi} \quad (A2)$$

Ignoring the Langer correction<sup>16</sup> for rotationless levels (i.e. using  $\phi$  values for  $\theta = 0$ , rather than for  $j = 0$ ),<sup>53</sup> one may obtain  $dK/d\phi$  by direct numerical interpolation.<sup>54</sup>  $\Delta G(v)$  values thus obtained, via Eq. (A2), yield curves B, C, D, and E in Fig. 8. The points on curve D are the exact quantal<sup>8</sup> vibrational spacings for this case,<sup>5</sup>  $\Delta G_{v+1/2}$ . Case A refers to a purely attractive potential  $V(R)=D-2/R^6$ ; curve A is generated by substituting Eq. (6) into Eq. (4), with  $n = 6$  and

$C_6 = 2.55$  The abscissa scales have been shifted to make all  $v_D$ 's coincide. The insert on Fig. 8 shows the five potentials of the same  $C_6$ .

The convergence of the different curves in Fig. 8 as the dissociation limit is approached is considered good evidence of the practical validity of the present method. Increases in reduced mass  $\mu$  and/or the depth or breadth of the potentials (introducing more vibrational levels) would merely stretch the ordinate and abscissa scales, and shift the lower curves up towards curve A (which would remain unchanged).

## Appendix B: Asymptotic Inverse-Power $\tilde{n}$ for Atomic Interactions

This section summarizes rules for determining the limiting asymptotic power  $\tilde{n}$  in the internuclear interaction. It is based on the references in footnotes 20, 41, 56, and 57, and is limited to first- and second-order perturbation theory results. Magnetic (or relativistic) effects are ignored; this is reasonable for  $R \lesssim 20$  a.u.<sup>58</sup> (and levels with outer turning points at larger distances would not be readily observed).

The  $\tilde{n}$  of the lowest order term in the inverse-power series expansion (Eq. 13) for the long-range internuclear potential is determined by the nature of the two atoms to which the molecular state adiabatically dissociates. If the two atoms are charged, of course  $\tilde{n} = 1$ ; if one is charged and the other is in an electronic state with a permanent dipole moment,<sup>59</sup>  $\tilde{n} = 2$ ; if both atoms are uncharged and in electronic states with permanent dipole moments,<sup>59</sup>  $\tilde{n} = 3$ . Another case in which  $\tilde{n} = 3$  occurs is in the interaction between two identical uncharged atoms in electronic states whose total angular momenta differ by one (i.e.,  $\Delta L = 1$ ); this interaction is a first-order dipole resonance,<sup>56</sup> and unlike the effects mentioned above, has no classical electrostatic analog. For interactions between a charged and a neutral atom,  $\tilde{n} = 4$  and  $C_4 = \frac{Z^2 e^2 \alpha}{2}$ , where  $Ze$  is the charge on the ion, and  $\alpha$  the polarizability of the neutral. The case  $\tilde{n}=4$  can also arise in the interaction of an atom with a permanent electric dipole moment,<sup>59</sup> and a non S-state atom with a permanent quadrupole moment.

In general, pairs of (uncharged) non S-state atoms have a first-order quadrupole-quadrupole interaction which corresponds to  $\tilde{n} = 5$ ,

and theoretical  $C_5$  values are available for a wide range of systems.<sup>41</sup> Occasionally the  $C_5$  coefficient for a particular state is zero for reasons of symmetry (eg., for the ground ( $X^1\Sigma_g^+$ ) state of the halogens<sup>36</sup>), and in this case  $\tilde{n} = 6$ . For states which do not fall into any of the above classifications,  $\tilde{n} = 6$  (since all interacting species are subject to the London induced dipole-induced dipole forces).

### Footnotes

1. R. T. Birge and H. Sponer, Phys. Rev. 28, 259 (1926).
2. R. T. Birge, Trans. Faraday Soc. 25, 707 (1929).
3. For a recent review see A. G. Gaydon, Dissociation Energies, 3rd Edition, Chapman and Hall Ltd., London (1968).
4. G. Herzberg, Molecular Structure and Molecular Spectra: I. Spectra of Diatomic Molecules, 2nd Edition, D. Van Nostrand Company, Inc., Toronto (1950).
5. Note that while  $\Delta G(v)$  is Herzberg's  $\Delta G_v$ ,  $\Delta G(v+\frac{1}{2}) = \frac{dE(v+\frac{1}{2})}{dv}$  is not identical to the "observable" vibrational level spacing  

$$\Delta G_{v+\frac{1}{2}} = \int_v^{v+1} \Delta G(v) dv \quad (\text{see p. 98 in Ref. 4}).$$
6. a) H. Harrison and R. B. Bernstein, J. Chem. Phys. 38, 2135 (1963);  
 b) Erratum 47, 1884 (1967).
7. See the review by E. A. Mason and L. Monchick, Advances in Chemical Physics, 12, 329 (1967), Interscience-Wiley, New York.
8. The parameters of the L.J.(12,6) potential were chosen to allow for 24 bound states. In the notation of Ref. 6, this corresponds to  $B_z = \frac{2\mu D_e R_e^2}{\hbar^2} = 10000.$ , where  $D_e$  is the well depth, and  $R_e$  the position of the potential minimum. Eigenvalues were calculated numerically and are accurate to  $10^{-7} D_e$ . This was done using a slightly modified form of the Cooley-Cashion program: J. W. Cooley, Math Computation 15, 363 (1961); J. K. Cashion, J. Chem. Phys. 39, 1872 (1963).
9. I. S. Gradshteyn and I. M. Ryzhik, Tables of Integrals Series and Products (§ 3.251, page 295) Academic Press, New York (1963).
10. M. Abramowitz and I. Stegun, Handbook of Mathematical Functions, U. S. Nat. Bur. Std. Appl. Math. Series 55. U. S. Dept. of

Commerce, Washington, D. C. (1964); also from Dover Publications Inc., New York (1965 ).

11. This is because a direct fit of experimental energies to Eq. (4) requires a prior numerical smoothing of the data to obtain accurate values of the derivatives  $\frac{dE(v)}{dv}$ .
12. It is interesting to note that for  $n = 4$  (ion-induced dipole forces) Eq. (6) is simply a quartic in  $v$ , and for  $n = 6$  (induced dipole-induced dipole, London dispersion forces) it is cubic.
13. By comparing Eq. (1) for  $E(v) = D$  and  $E(v)$  at a slightly smaller  $v$ , W. C. Stwalley (private communication, 1969) independently obtained a result for  $n = 6$  which, upon generalization for any  $n > 2$ , may be cast into the useful form of Eq. (6). However, his factor equivalent to the present  $K_n$  is slightly less general, and this approach (unlike the present one) cannot be applied to cases with  $n \leq 2$ . While seeking a "natural" analytic expression to describe the vibrational spectrum of  $H_2$ , C. L. Beckel (J. Chem. Phys. 39, 90 (1963)) proposed empirical formulae somewhat similar in form to Eq. (6).
14. P. M. Morse and H. Feshbach, Methods of Theoretical Physics, Vol. II ( § 12.3), McGraw-Hill, New York (1953).
15. For pure inverse-power potentials with  $n > 2$ , there are a finite number of levels within any finite neighborhood of the dissociation limit, but there are an infinite number of discrete levels below it, extending down to infinite binding energy. For potentials with  $n < 2$  there exists a lowest level bound by a finite energy, while there are an infinite number of levels within any finite neighborhood

of  $D$ . For  $n = 2$  the levels extend down to infinite binding energy, and there are an infinite number of levels in any finite neighborhood of  $D$ .

16. R. E. Langer, Phys. Rev. 51, 669 (1937). The Langer correction (i.e., replacing  $j(j+1)$  by  $(j+\frac{1}{2})^2$ ) would require replacing Eq. (3a) by:  $V(R) = D - \frac{C_n}{R^n} + \frac{\hbar^2}{2\mu} \frac{1}{4R^4}$ . For  $n = 2$  this just means that  $C_2$  in Eq. (7) becomes  $(C_2 - \frac{\hbar^2}{8\mu})$ , but for  $n \neq 2$  the integral arising from Eq. (2) is no longer analytically soluble. However, for realistic systems the Langer correction is fortunately very small.
17. Within the context of the present approach, potentials with exponential long-range tails (such as the Morse potential) correspond qualitatively to inverse-power potentials with very large  $n$ . The purely attractive exponential potential has both a discrete lowest level and a finite number of bound states within any finite neighborhood of  $D$ .
18. A linear B-S plot for levels near the dissociation limit of a potential will be considered as an indication that the potential in the given region is effectively exponential in form.
19. Care should be taken to avoid confusion between the well depth  $D_e$ , and  $D$ , the position of the dissociation limit.
20. See the discussion of intermolecular forces in
  - a) Molecular Theory of Gases and Liquids by J. O. Hirschfelder, C. F. Curtiss and R. B. Bird, John Wiley and Sons, New York (1964).
  - b) J. O. Hirschfelder and W. J. Meath, Advances in Chemical Physics, XII, (Intermolecular Forces), 1 (1967), Interscience, New York.

21. Note that in the case where some of the dominant terms in Eq. (13) are repulsive (ie., their  $C_m < 0$ ), some of these weighting factors will have differing signs, and the resulting value of  $n$  may then lie outside the range of the  $m$ 's of the contributing terms. If the lowest inverse-power term is repulsive while the higher power terms are attractive, this gives rise to a potential maximum at large  $R$ . This appears to be the case for the  $^3\Pi_{0g}^+$  state of  $I_2$ : R. J. LeRoy, J. Chem. Phys. 52, 0000 (1970).
22. In this context a potential is "well behaved" if it has no potential maximum and no non-adiabatic perturbation.
23. Of course both errors approach zero for levels approaching  $D$ .
24. a) See, eg., the discussion by J. K. Cashion, J. Chem. Phys. 48, 94 (1968); see also Appendix A.  
 b) A. S. Dickinson, private communication (1968).
25. See Appendix B for a summary of the theoretical  $\tilde{n}$  values for a wide variety of cases.
26. Non-linear least-squares regression computer programs for fitting arbitrary analytic functions are available at most computing centers. The present calculations used the University of Wisconsin Computing Center subroutine GASAUS for such fits.
27. Primes denote differentiation with respect to  $v$ ; eg.,  
 $E'(v) \equiv dE(v)/dv$ .
28. Parameter values obtained from Eqs. (15) and (16) should, in principle, be just as reliable as those obtained from Eq. (6). However, the former approach requires a prior smoothing of the data to obtain accurate values of the derivatives  $^{27} E'(v)$  and  $E''(v)$ , and in practice

this introduces some error. Experience has shown that while trial parameter values from Eqs. (15) and (16) are satisfactory, they are measurably improved by four parameter fittings to Eq. (6).<sup>26</sup>

29. In all of the results presented, an initial fit of the data to Eqs. (15) and (16) yielded trial parameter values which were used to initiate the general non-linear fit to Eq. (6).<sup>26,30</sup>
30. R. J. LeRoy and R. B. Bernstein, University of Wisconsin Theoretical Chemistry Institute report WIS-TCI-369 (1969), to be published. The report contains in an appendix Fortran listings of the programs used for carrying out fits to Eq. (6), (15), and (16).
31. This is mainly because of the problem of averaging the estimates of  $D$  and  $K_n$  obtained at different values of  $v$ , to yield a mutually consistent set of parameters. It is interesting that analogous to Eq. (17),

$$n = \frac{4[E''(v)]^2}{E'(v)E'''(v)} - 2$$

but because of the above problem this expression is less reliable than is Eq. (15).

32. Since the derivatives are obtained from the highest 11 energies only, they cannot be accurate at the end points, so only the 9 points shown on Fig. 2 are reliable.
33. Since the input data (level energies) are never completely error-free, a given fit should always utilize at least one level more than the number of free parameters being fitted. If there is significant experimental uncertainty in the energies (eg., more than a few percent of the level spacings) a redundancy of more than one level may be required to yield meaningful values of the parameters.

34. In the application of this method to the  $B^3\Pi_{Ou}^+$  state of  $I_2^{30}$ , the experimental uncertainty introduces considerable imprecision into the four-parameter fits, so that  $n$  could not be directly determined within required accuracy of better than  $\pm 1$ . However, comparison of the  $D$  curves yielded by three-parameter fits with  $n$  fixed different trial values, strongly suggested that  $\tilde{n} = 5$ .
35. D. E. Stogryn and J. O. Hirschfelder, J. Chem. Phys. 31, 1531 (1959). These authors derived an analytic expression (their Eq. (89)) for the exact first-order WKB value of  $v_D$  (which omits the effect of the the Langer correction<sup>16</sup>). A more exact value of the numerical constant in their Eq. (92) is 1.6826.
36. A. E. Douglas, Chr. Kn. Møller and B. P. Stoicheff, Can. J. Phys. 41, 1174 (1963).
37. The experimental data for this system are for the most common isotope  $^{35,35}Cl_2$ ; all energies are expressed relative to the  $v'' = 0, J'' = 0$  level of its ground electronic state.
38. T. Y. Chang, Mol. Phys. 13, 487 (1967); see also the discussion in Appendix B.
39. M. A. Byrne, W. G. Richards and J. A. Horsley, Mol. Phys. 12, 273 (1967).
40. In choosing these values it is assumed that the "hook" at the end of the  $n = 5$  curves in Fig. 5 is significant, illustrating the decrease of the error term for levels farther into the asymptotic ( $n = \tilde{n}$ ) region. The indicated uncertainties (including the error bars in Fig. 5) correspond to one standard error in the fitted parameters and are smaller than the probable error limits.

41. It has been shown by J. K. Knipp (Phys. Rev. 53, 734 (1938)) that  $C_5$  coefficients may be expressed as a product of an angular factor and  $[\langle r_A^2 \rangle \langle r_B^2 \rangle]$ , the product of the expectation values for the square of the electron radii in the unfilled valence shells on interacting atoms A and B. Knipp presented values of the angular factors and approximate expectation values for a few systems, and T. Y. Chang (Rev. Mod. Phys. 39, 911 (1967)) extended these results considerably. Recently C. F. Fischer (Can. J. Phys. 46, 2336 (1968)) has reported Hartree-Fock values of  $\langle r^2 \rangle$  for all shells of atoms from He to Rn.
42. The erratic nature of the curve in Fig. 6 is due to the influence of small errors in the experimental energies on the fitted values of the parameters; the corresponding values of  $n$ ,  $C_n$ , and  $v_D$  show similar behavior. Including more levels in each fit dampens these oscillations.
43. Holding  $D$  fixed dampens the "noise" due to experimental uncertainty,<sup>42</sup> yielding a more reliable segmented potential.
44. J. A. C. Todd, W. G. Richards, and M. A. Byrne, Trans. Faraday Soc. 63, 2081 (1967).
45. For a somewhat related discussion of the quasibound states, see A. S. Dickinson and R. B. Bernstein, Mol. Phys. (to be published).
46. While the present method is expected to give values of  $C_n$  which are slightly small (see Sec. IIB), there is reason to suspect that the theoretical  $C_5$  value used for comparison<sup>41</sup> may be somewhat too large. M. T. Marron (private communication, 1969) points out that Fischer's<sup>41</sup> values of  $\langle r^2 \rangle$  are based on Hartree-Fock

wave functions which do not have correct asymptotic tails, and that correcting for this may decrease  $\langle r^2 \rangle$ , and hence the theoretical  $C_5$ .

47. For a few systems, such as isotopic hydrogen and most hydrides, the inverse-power long-range forces are relatively weak, so that the B-S plot shows negative or zero curvature even for the very highest levels.
48. R. B. Bernstein, Phys. Rev. Lett. 16, 385 (1966).
49. J. A. Horsley and W. G. Richards. J. Chim. Phys. 66, 41 (1969).
50. See, for example, H. Pauly and J. P. Toennies, Chapt. 3.1 (p. 227) of Methods of Experimental Physics, L. Marton, Ed., Vol. 7 of Atomic and Electron Physics: Atomic Interactions, Part A, Academic Press, New York (1968).
51. Although all of the cases thus far considered correspond to  $\tilde{n} = 5$  or 6, the present method should be even more successful for systems with smaller  $\tilde{n}$  (eg.,  $\tilde{n} = 4$ , for molecules which dissociate to ion+neutral) because of the relatively higher density of levels near  $D$ .
52. The present work utilized the corrected tables reported in Ref. 6b. These are available as Document No. 9499 in the ADI Auxiliary Publications Project, Photoduplication Service, Library of Congress, Washington, D. C. 20540.
53. Comparison of the  $\phi$  values<sup>6,52</sup> for  $\theta = 0$  and, say,  $\theta = 10^{-4}$  shows that this introduces negligible error.
54. This was done by piecewise fitting of third-order polynomials in  $\phi$ . Despite the rather large gaps between the tabulated points

for large  $\phi$ , this is expected to be fairly accurate since the eigenvalue distribution for the highest levels of an  $R^{-6}$ -tailed potential is expected to be cubic in  $v$  (i.e., in  $\phi$ ).<sup>12</sup>

55. Although the exact  $v_D$  is infinite for the pure  $R^{-6}$  attractive potential, there are a finite number of levels within any finite interval about  $D$ .<sup>15</sup> Hence the quantities  $(v_D - v)$  and curve A in Fig. 8 are significant in the semiclassical (WKB) approximation.
56. G. W. King and J. H. Van Vleck, Phys. Rev. 55, 1165 (1939).
57. H. Margenau, Rev. Mod. Phys. 11, 1 (1939).
58. This conclusion is partly based on Chang's conclusion<sup>41</sup> that for the  $0_g^+$  states of  $O_2$  and  $Cu_2$ , these effects do not dominate the interaction until  $R > 60a.u.$
59. This case is, however, relatively uncommon; Hirschfelder and Meath<sup>20a</sup> point out that only an excited H atom can have a permanent dipole moment.

### Legends for Figures

- Fig. 1. Exact integrand (solid curves) of Eq. (2) for three levels of a "standard" 24-level L.J.(12,6) potential.<sup>8</sup> The dashed segment of curve near  $R_1$  is the approximate integrand  $[E(v) - (1 - 2/R^6)]^{-1/2}$  for  $v = 20$ . The dashed vertical lines are the turning points, where the exact integrand is singular.
- Fig. 2.  $E'(v)/E''(v)$  vs.  $v$  for the highest levels of the 24-level L.J.(12,6) potential.<sup>32</sup> The broken lines have slopes corresponding to integer  $n = 5, 6$ , and  $7$  (see Eq. (15)).
- Fig. 3. Results of fitting Eq. (6) to the vibrational levels of the 24-level L.J.(12,6) potential.<sup>8,26,29</sup> The points correspond to fits of levels  $v_L$  up to  $v_H = 23$ . The broken horizontal lines denote the exact quantities  $\tilde{n} = 6$ ,  $D = 1.0$ , and  $C_6 = 2.0$ . The "best"  $n = 6$  estimate of  $v_D$  is 23.353, in good agreement with the value 23.358 generated from the analytic expression of Stogryn and Hirschfelder.<sup>35</sup> Points joined by solid lines correspond to four-parameter fits with  $n$  being varied freely, while the others correspond to three-parameter fits with  $n$  held fixed at the indicated values.
- Fig. 4. Piecewise potentials constructed from three-parameter fits ( $D$  constrained at 1.0) of the L.J.(12,6) vibrational energies<sup>8</sup> to Eq. (6).<sup>26,29</sup>  $\odot$  exact turning points for the specified levels; — segments obtained from fits; --- exact asymptotic  $R^{-6}$  potential tail.

Fig. 5. Results of fitting Eq. (6)<sup>26,29</sup> to the experimental vibrational energies of  $\text{Cl}_2(\text{B}^3\Pi_{0u}^+)$ .<sup>36,37</sup> The points correspond to fits of levels  $v_L$  up to  $v_H = 31$ . The broken vertical line is the best estimate obtained for  $D$ . Points joined by solid curves correspond to four-parameter fits with  $n$  varied freely, while the others correspond to three-parameter fits with  $n$  held fixed at the indicated values.

Fig. 6.  $D$  estimates obtained by fitting Eq. (6) to the energies of levels  $v_L$  to  $v_H$ ,<sup>26,29</sup> where  $v_H - v_L = 7$  and  $v_H$  is varied. The vertical and horizontal broken lines denote the best present estimate of  $D$ .

Fig. 7. Piecewise potentials constructed from three-parameter fits (with the constraint  $D = 20879.75 \text{ cm}^{-1}$ ) of the experimental vibrational energies<sup>36</sup> of  $\text{Cl}_2(\text{B}^3\Pi_{0u}^+)$  to Eq. (6).<sup>26,29</sup>  
 ⊙ RKR turning points for the specified levels;<sup>44</sup>  
 — segments obtained from fits.

Fig. 8. Birge-Sponer plots for various (L.J.(12,6), Exp( $\alpha$ ,6) and pure  $R^{-6}$ ) potentials with the same long-range tail; the insert shows the corresponding potential curves. A: pure  $R^{-6}$ ,  $V(R) = D - C_6/R^6$ ; B, C, and E: Exp( $\alpha$ ,6), see Table II; D: "model" L.J.(12,6).<sup>8</sup> All B-S curves except A were generated from Eq. (A2) using WKB integral tables;<sup>6,52</sup> the points are exact quantal level spacings for the L.J.(12,6) case,<sup>8</sup> and they confirm the accuracy of the WKB approximation.<sup>5</sup> Curve A was obtained on substituting Eq. (6) into Eq. (4).<sup>55</sup>

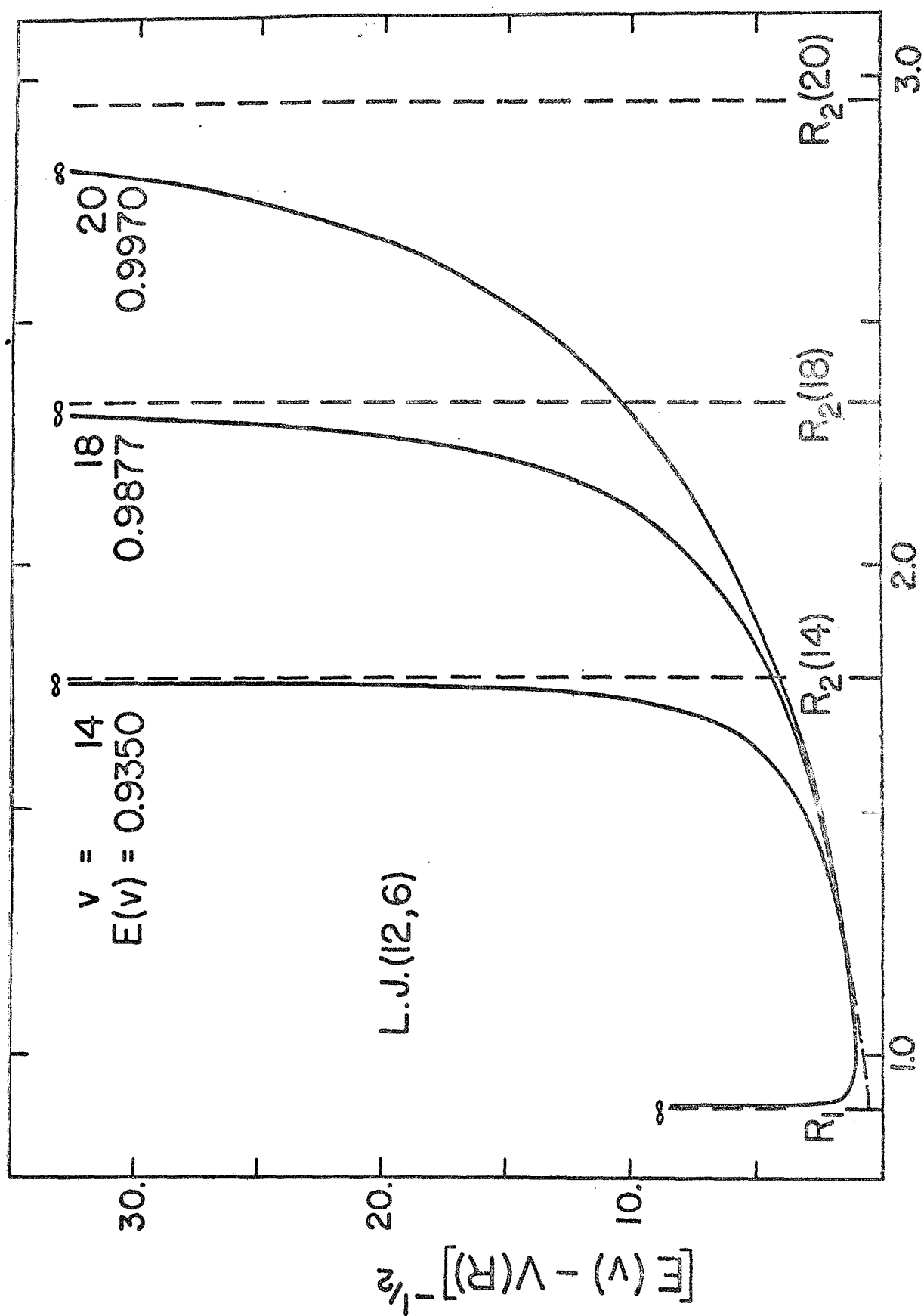


Fig. 1

100  
100  
100

100

100

100

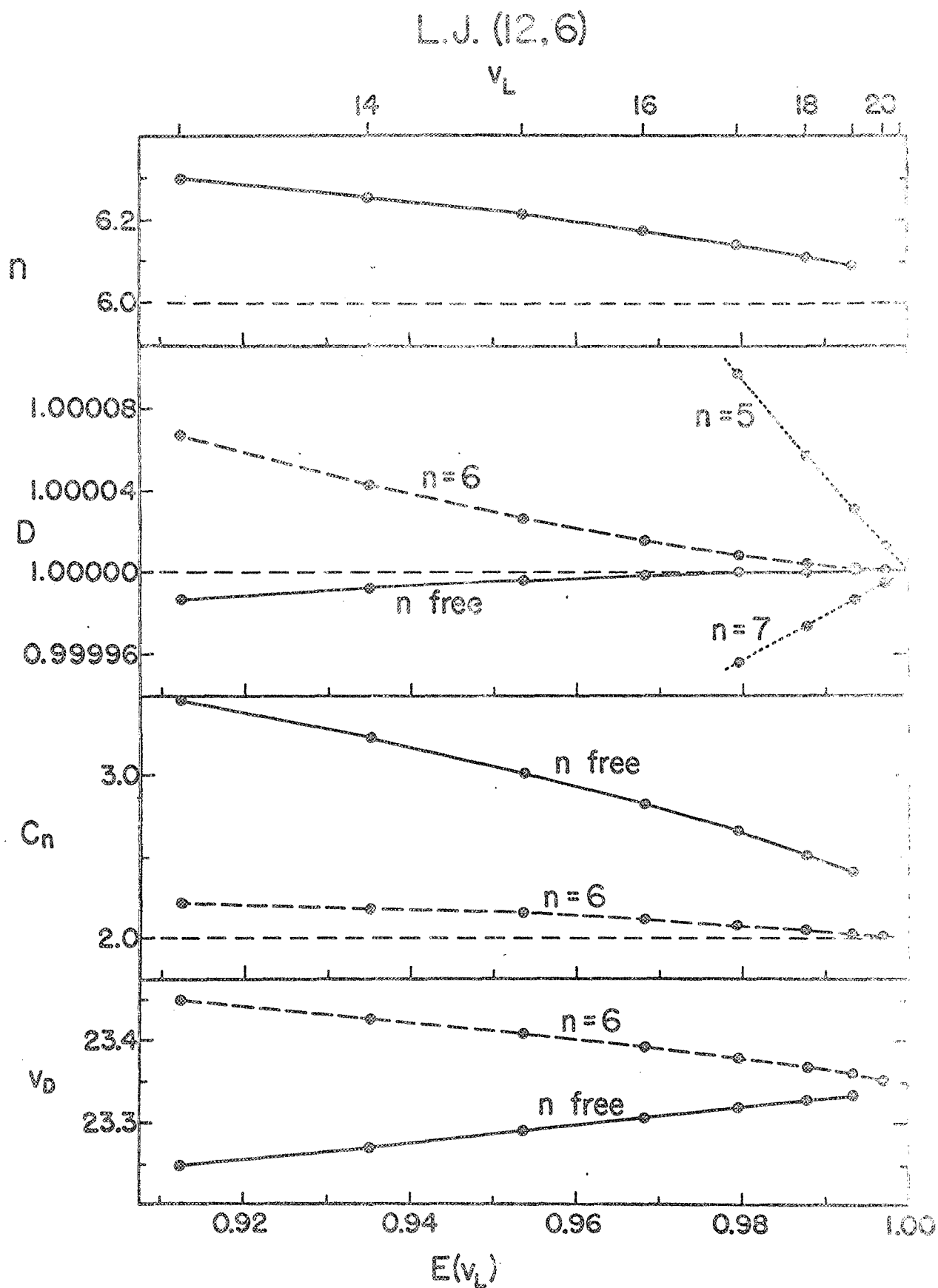


Fig. 3

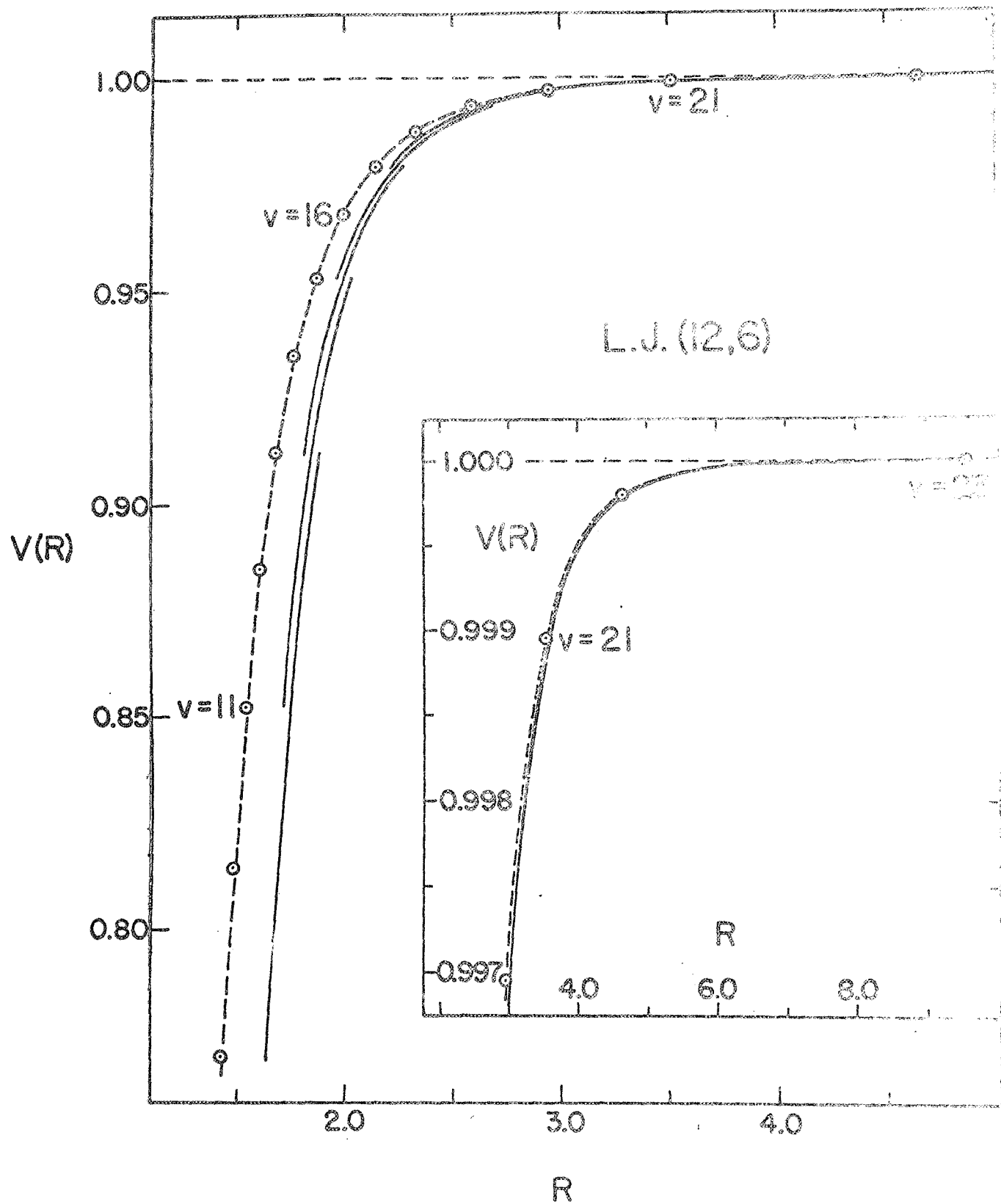


Fig. 4

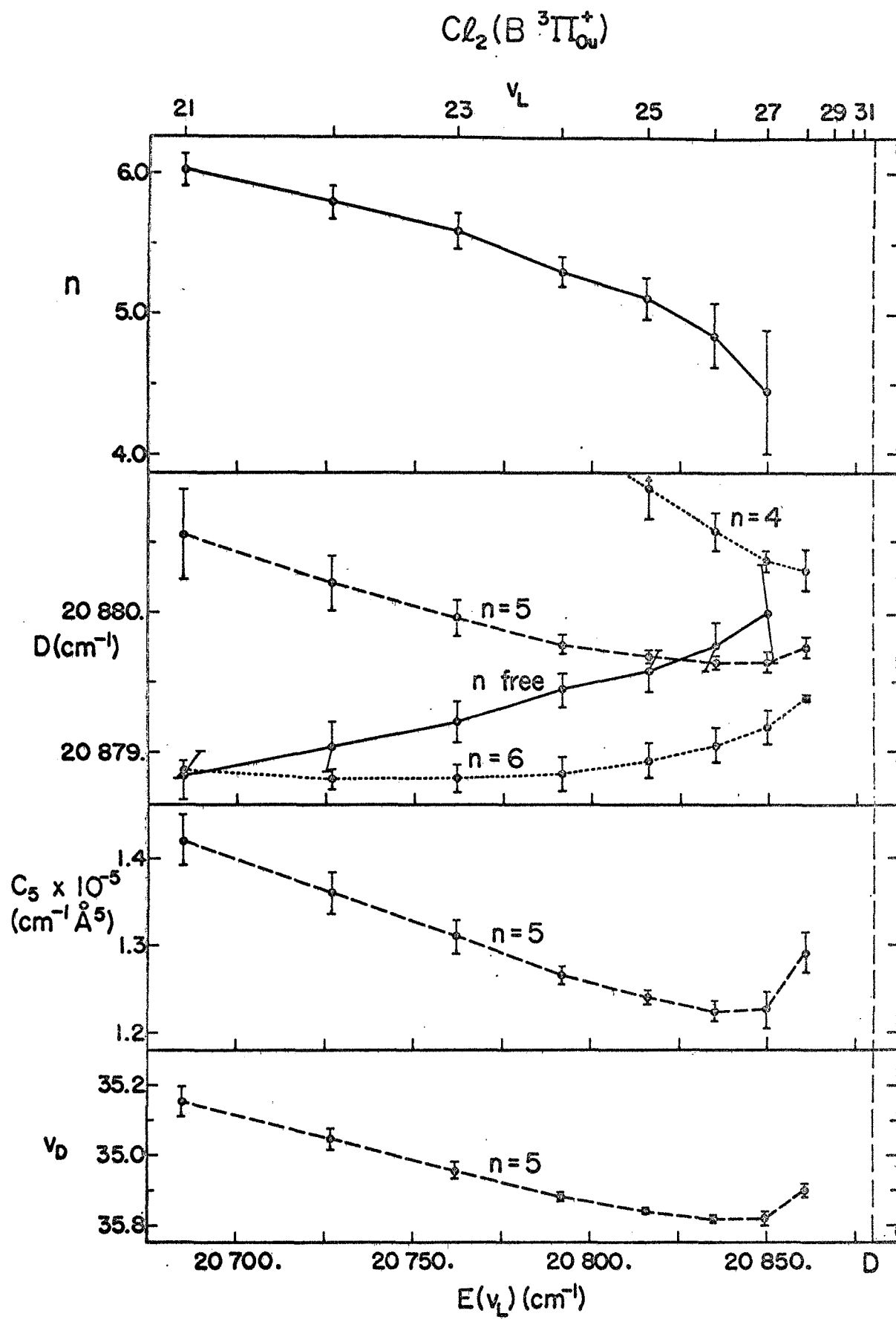
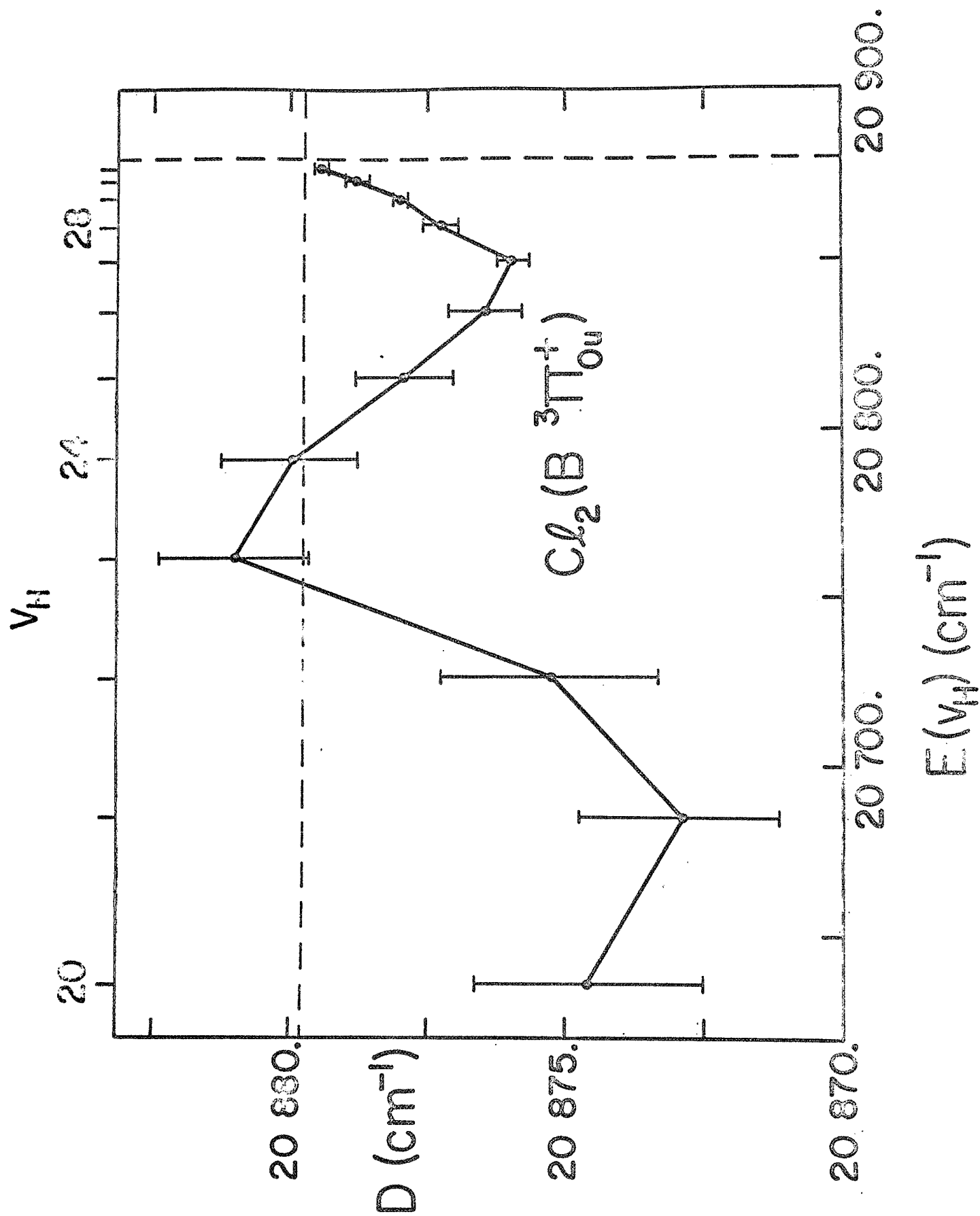


Fig. 5



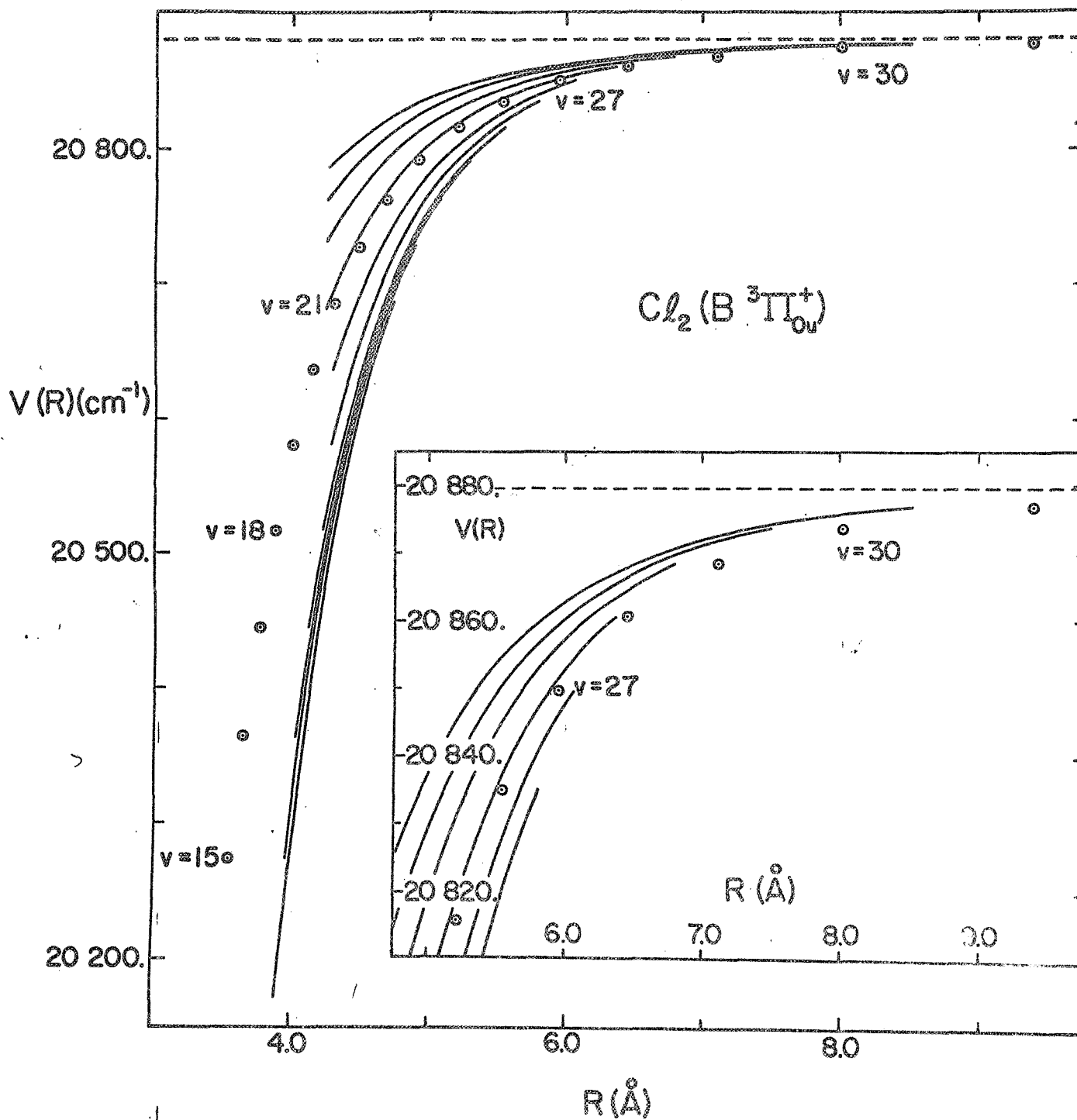


Fig. 7.

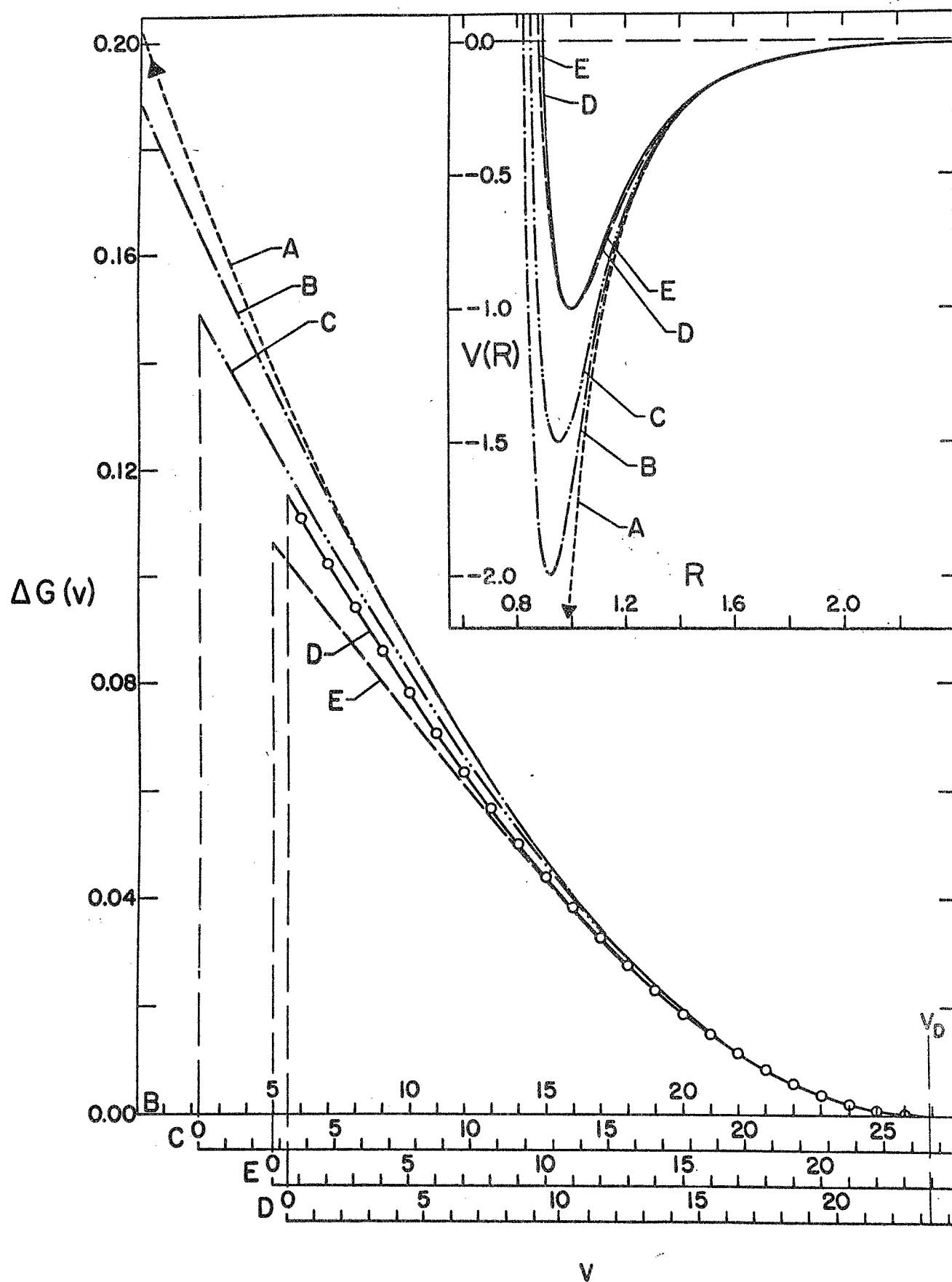


Fig. 8